Agriculture, Ecosystems and Environment xxx (2014) xxx–xxx

Contents lists available at ScienceDirect

Agriculture, Ecosystems and Environment

journal homepage: www.elsevier.com/locate/agee

Iron oxides as proxies for characterizing anisotropy in soil CO_2 emission in sugarcane areas under green harvest

Angélica Santos Rabelo de Souza Bahia[a,*], Marques José Jr[a], Alan Rodrigo Panosso[b], Livia Arantes Camargo[a], Diego Silva Siqueira[a], La Scala Newton Jr[a]

[a] Agrarian and Veterinarian Faculty, São Paulo State University (FCAV/UNESP), Via de Acesso Prof. Paulo Donato Castellane s/n, 14883-292 Jaboticabal, SP, Brazil
[b] Ilha Solteira Engineering Faculty, São Paulo State University (FEIS/UNESP), Avenida Brasil 56, Centro15385-000, Ilha Solteira, SP, Brazil

ARTICLE INFO

Article history:
Received 27 August 2013
Received in revised form 11 April 2014
Accepted 18 April 2014
Available online xxx

Keywords:
Diffuse reflectance spectroscopy
Soil respiration
Hematite
Goethite
Geostatistics
Multivariate analysis

ABSTRACT

Soil CO_2 emission (FCO_2) is a main contributor of atmospheric carbon transfer and is the subject of research aimed at developing effective methods for characterizing and mitigating CO_2 emissions. The FCO_2 is related to various soil properties including porosity, density and moisture, which are in turn related to gas transfer, O_2 uptake and CO_2 release, as well as mineralogical components (particularly iron oxides, which are closely associated with aggregation and protection of soil organic matter). As estimated by diffuse reflectance spectroscopy (DRS), soil iron oxides such as hematite (Hm) and goethite (Gt) can be useful in determining FCO_2. The main objective of this experiment was to assess the usefulness of the mineralogical properties Hm, Gt, and iron oxides extracted by dithionite–citrate–bicarbonate (Fe_d) to estimate the FCO_2 in a sugarcane area under green harvest in southeastern Brazil. The experiment was conducted using an irregular 50 m × 50 m grid containing 89 sampling points 0.50–10 m apart to assess the soil properties. The FCO_2 at each sampling point was measured at the beginning of crop growth and 54 days after planting with the use of two portable LI-COR LI-8100 Soil CO_2 Flux Systems. The soil properties studied were found to be spatially dependent and exhibited well-defined anisotropy (particularly the mineralogical properties Hm, Gt and Fe_d). The first two components of a principal component analysis (PC1 and PC2) jointly accounted for 73.4% of the overall result variability with PC1 essentially related to the physical and mineralogical properties of the soil. Based on a multiple linear regression analysis, free water porosity (FWP) and Hm accounted for 71% of the FCO_2 variability. Our results indicate that soil preparation and management practices in mechanically harvested sugarcane affect some factors inherent in the soil forming processes, including physical and mineralogical properties, which in turn affect FCO_2. These results affirm the potential of DRS as an auxiliary tool for determination of properties that are typically associated with FCO_2. In addition, the ensuing method allows for large-area FCO_2 mapping to developing greenhouse gas emission inventories for agricultural soils.

1. Introduction

Researchers throughout the world are investigating global climate change variables with a hope of reversing them and preventing their adverse impacts on the planet (FAPESP, 2008). Such investigations include quantifying greenhouse gases in agricultural areas (Dasselaar et al., 1998; Xu and Qi, 2001; Kosugi et al., 2007; Konda et al., 2010; Boeckx et al., 2011; Allaire et al., 2012), and particularly in tropical regions (Cerri et al., 2007; La Scala et al., 2009; Teixeira et al., 2011; Panosso et al., 2012), where the physical, chemical and biological processes are especially intense (Andreae and Crutzen, 1997).

For example, researchers have devised methods to quantify soil to atmosphere CO_2 emissions (FCO_2) in hopes of developing effective methods for inventorying greenhouse gas emissions (Cerri et al., 2007, 2009; Singh et al., 2010; De Figueiredo and La Scala, 2011). The portable system for assessing FCO_2 is impractical for use in large areas since the available sampling time is relatively short because substantial differences in temperature between measurements, and hence the potential effects of temporal variability in FCO_2 which is influenced by soil temperature (Teixeira et al., 2011), must be avoided.

* Corresponding author. Tel.: +55 1632092601; fax: +55 16 32092601.
E-mail addresses: angelicasantosrabelo@yahoo.com.br, angelagro2005@hotmail.com (A.S.R.S. Bahia).

http://dx.doi.org/10.1016/j.agee.2014.04.017
0167-8809/

Diffuse reflectance spectroscopy (DRS) is a potentially useful auxiliary tool for conventional laboratory work (Viscarra Rossel et al., 2006). Soil property estimates provided by the DRS technique are especially accurate and can be obtained in an easy, timely, and economical manner relative to traditional methods (Janik et al., 1998; Barrón et al., 2000; Demattê et al., 2006; Torrent and Barrón, 2008). Furthermore, DRS is a non-polluting technique and uses no chemicals.

In combination with chemometric techniques, the use of DRS in visible (300–800 nm) and near-infrared (800–2500 nm) spectral regions has facilitated the determination of mineralogical soil properties (Janik et al., 1998; Viscarra Rossel et al., 2006; Viscarra Rossel and Webster, 2011). Thus, some bands in the visible spectral region are related to iron oxides such as hematite (Hm) and goethite (Gt) (Scheinost et al., 1998), which are ubiquitous in tropical soils. La Scala et al. (2000) found significant correlation between soil respiration and the soil's content of organic carbon and iron extracted from clay, which are closely related to soil spectral reflectance (Demattê et al., 2006; Viscarra Rossel and Webster, 2011). The prevalence of iron oxides in highly weathered soils, such as in Brazilian Latosols, makes the spectral properties of soil CO_2 emission even more useful for characterization purposes.

Some researchers have observed a high spatial variability in FCO_2 and its governing soil properties (La Scala et al., 2000; Xu and Qi, 2001; Epron et al., 2006; Kosugi et al., 2007; Allaire et al., 2012; Camargo et al., 2013). Such variability can even differ between the directions of the crop planting line (La Scala et al., 2009; Martin and Bolstad, 2009; Panosso et al., 2012). This phenomenon, known as "spatial anisotropy", has been ascribed to various soil formation factors but particularly io relief (Epron et al., 2006; Brito et al., 2010) and agricultural management practices (Carvalho et al., 2002; Panosso et al., 2012). In fact, soil preparation and management practices can alter the soil property spatial variability structure influencing FCO_2 in different directions (Panosso et al., 2012), which are in turn, directly related to agricultural environment carbon dynamics (Benbi and Brar, 2009; La Scala et al., 2009; Boeckx et al., 2011; Allaire et al., 2012; Herbst et al., 2012).

Although the spatial assessment of soil properties is widely documented, studies on spatial anisotropy in soil CO_2 emission and, particularly, of mineralogical properties, are scarce. This work was undertaken to confirm our hypothesis that estimates of mineralogical properties obtained by diffuse reflectance spectroscopy (DRS) can be effective proxies for charactering anisotropy in soil CO_2 emission. The primary aim was to assess hematite and goethite content estimated by DRS to identify FCO_2 anisotropy in a green-harvested sugarcane area in southeastern Brazil.

2. Materials and methods

This study was a continuation of previous work carried out by Panosso et al. (2012) on the fractal characterization of FCO_2 anisotropy in a green-harvested sugarcane area. The experimental plot was located in Guariba, São Paulo, Brazil (21°24′S, 48°09′W) at 550 m above sea level. The soil was a eutroferric Red Latosol (Haplustox, USDA Soil Taxonomy) of a highly clayey texture on a 3% slope. The study was conducted on an irregular 50 m × 50 m sampling grid containing 89 points that were 0.50–10 m apart (Fig. 1). Soil samples were collected from each of these 89 points at the 0.00–0.10 m soil layer and subjected to physical, chemical, mineralogical, and spectral analysis. Sampling points were set in various directions with respect to the crop planting lines, namely: 0° (22 points aligned between consecutive planting lines); 90° (22 points normal to the harvest line); and 45° and 135° (22 points each in the soil preparation directions used to remove the left-over cane stubble from the previous 6 years). As seen in Fig. 1, the sampling grid consisted of 04 transects containing 22 points each along the above-described directions.

Soil CO_2 emission (FCO_2) was measured using two portable LI-COR LI-8100 systems at the beginning of crop growth and 54 days after planting. This portable system uses an optical absorption spectrophotometer to monitor changes in CO_2 concentration inside a chamber. The chamber, which is a closed system of 854.2 cm^3 inner volume and a circular soil contact of 83.7 cm^2, was placed on PVC soil collars previously inserted 3 cm deep at each of the 89 sampling points. To avoid further root respiration into the FCO_2, measurements were performed between crop lines. Soil temperature (T_s) was monitored using a 20 cm thermistor-based probe inserted 5 cm into the soil near the collars. Soil moisture (M_s) was expressed as percent volume, and was recorded with a portable hydrosense system (TDR probe, Campbell, USA). The FCO_2, T_s and M_s were measured in the early morning (07:00–08:30 am) and late afternoon (04:00–05:30 pm) in order to prevent soil temperature and moisture marked changes from affecting FCO_2. Mean FCO_2, T_s and M_s values were obtained from each of the four-day measurement.

Soil bulk density (D_s) was determined in undeformed samples collected in cylinders with an average of 4.0 cm high × 5.0 cm i.d. (EMBRAPA, 1997). Total pore volume (TPV) was determined in undisturbed soil samples that were soaked in a pan filled two-thirds with water for 48 h. The samples were then drained in a porous plate under a 60 cm saturated water pressure column (EMBRAPA, 1997). The free water porosity (FWP) fraction was calculated as the difference between total pore volume (TPV) and the fraction filled by water, which is equivalent to soil moisture (M_s): FWP = TPV − M_s.

The fraction of pedogenic iron extracted by dithionite–citrate–bicarbonate (Fe_d) was determined according to Mehra and Jackson (1960) and the amount of iron extracted by ammonium oxalate (Fe_o), which according to Camargo et al. (1986), is associated with poorly crystalline pedogenic iron oxides.

Mineralogical properties were estimated by diffuse reflectance spectroscopy (DRS) of fine, air-dried earth samples (TFSA) (particle diameter < 2.0 mm) (Torrent and Barrón, 2008). To this end, 1 g of soil was ground to uniform color in an agate mortar and placed in a cylindrical specimen holder 16 mm in diameter.

Reflectance spectra were obtained using a Lambda 950 UV/vis/NIR spectrophotometer (Perkin Elmer) with a 150 mm integrating sphere. Spectra were acquired over a range of 380–780 nm with 0.5 nm intervals (i.e., in the visible region). DRS provided the proportions of hematite and goethite, which were used to calculate the soil content of these minerals.

The Hm and Gt contents were estimated from the second derivative of the Kubelka–Munk function (Kubelka and Munk, 1931) for the DRS data according to Scheinost et al. (1998):

$$f(R) = \frac{(1-R)^2}{2R} \quad (1)$$

where R is the diffuse reflectance of the sample. Thereafter, were determined amplitudes of the spectral bands associated with the minerals Gt and Hm, according Scheinost and Schwertmann (1999).

The second-derivative curves obtained were used to identify the typical absorption bands for iron oxides (Kosmas et al., 1984; Scheinost et al., 1998). Goethite (Gt) was identified from wavelength bands that ranged from 415–425 to 440–450 nm, and hematite (Hm) from bands that ranged from 530–545 to 575–590 nm. The amplitudes (i.e., the distances between the minimum and maximum values) of the absorption spectra of goethite (A_{Gt}) and hematite (A_{Hm}) (Fig. 2) were used to calculate the proportions of Hm and Gt, and hence the concentrations of these minerals. The specific methods and applications used are described in greater detail elsewhere (Barrón et al., 2000; Torrent and Barrón, 2008).

The bands in the spectral regions of goethite and hematite were correlated with the contents in the two minerals as determined

Please cite this article in press as: Bahia, A.S.R.S., et al., Iron oxides as proxies for characterizing anisotropy in soil CO_2 emission in sugarcane areas under green harvest. Agric. Ecosyst. Environ. (2014), http://dx.doi.org/10.1016/j.agee.2014.04.017

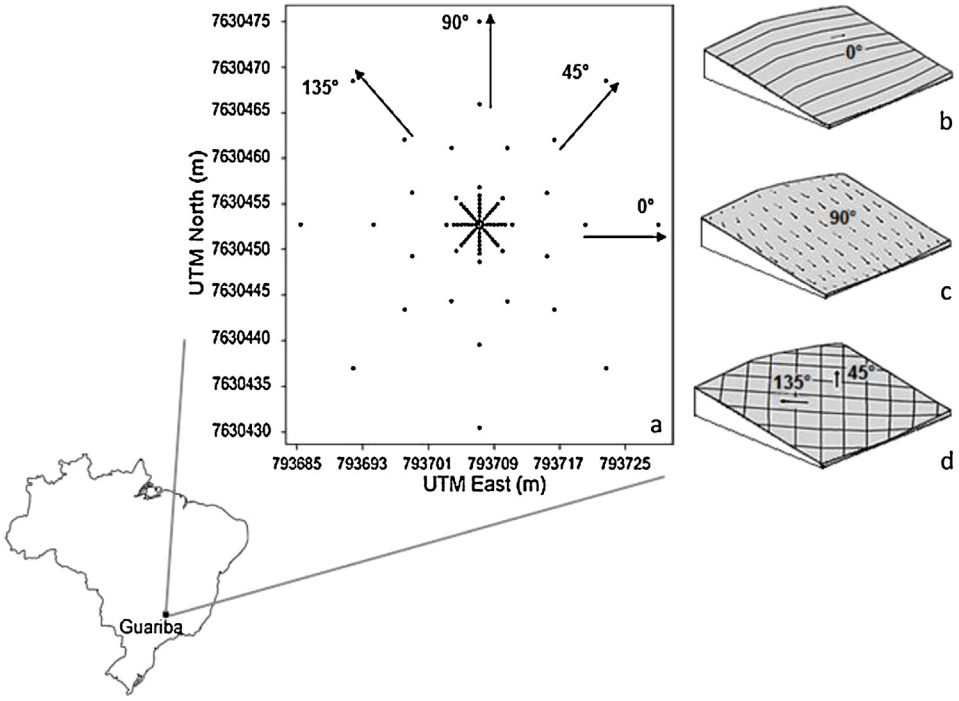

Fig. 1. Study area. (a) Location of the 89 points in the 50 m × 50 m grid; (b) Location of the points lined up between two planting lines; (c) Perpendicular to the planting line; (d) 45° and 135° were the directions of tillage used for 6 years to eliminate ratoon crops.

by X-ray diffraction (Scheinost et al., 1998). Regression analysis between oxide contents, as determined by X-ray diffraction spectroscopy and DRS, confirmed the positive correlation between the results of these two methods for hematite ($r = 0.97$, $p < 0.01$) and goethite ($r = 0.97$, $p < 0.01$). According to Kosmas et al. (1984), DRS can measure untreated soil samples because soil properties are not altered by any type of pretreatment.

Descriptive statistics was applied using SAS v. 9.0 software (SAS Institute, Cary, NC, USA). Analysis of variance (ANOVA) was used to compare the soil properties in different directions of the sampling grid. Spatial variability of the properties was assessed with geostatistical analysis (Webster and Oliver, 1990) in accordance with the principles of the intrinsic hypothesis. The semivariance at a given distance h was calculated from:

$$\hat{\gamma}(h) = \frac{1}{2N(h)} \sum_{i=1}^{N(h)} [z(x_i) - z(x_i + h)]^2 \quad (2)$$

where $\hat{\gamma}(h)$ is the experimental semivariance a separation distance h; $N(h)$ is the number of point pairs a distance h, $z(x_i)$ the value of variable z at point x_i; and $z(x_i + h)$ is the value of variable z at point $x_i + h$. A variogram describes spatial continuity or dispersion in the variables as a function of the distance between two locations (Deutsch and Journel, 1998). We used a minimum of 56 pairs of points to construct the variograms. Wollenhaupt et al. (1997), Journel and Huijbregts (1978), and Guerra (1988) recommend using at least 30 pairs to accurately estimate semi-variances, whereas Chilès and Delfiner, 1999 recommend using at least 50.

Spatial variability patterns are usually established using isotropic models (Konda et al., 2010; Teixeira et al., 2011; Allaire et al., 2012; Herbst et al., 2012) which ignore potential variability in different directions. However, agricultural management practices are known to introduce anisotropy in soil properties (La Scala et al., 2000, 2009). This led us to characterize the structure of spatial variability and its dependence on the target soil properties by using isotropic and anisotropic variograms that were fitted to two different types of theoretical models, namely:

(a) Spherical model:

$$\begin{cases} \hat{\gamma}(h) = C_0 + C_1 \left[\frac{3}{2} \left(\frac{h}{a} \right) - \frac{1}{2} \left(\frac{h}{a} \right)^3 \right]; & \text{if } 0 < h < a \\ \hat{\gamma}(h) = C_0 + C_1; & \text{if } h \geq a \end{cases} \quad (3)$$

(b) Exponential model:

$$\hat{\gamma}(h) = C_0 + C_1 \left[1 - \exp\left(-3 \frac{h}{a} \right) \right]; \quad \text{if } 0 < h < d \quad (4)$$

where d is the maximum distance in the variogram.

The parameters defining the models are known as nugget effect (C_0), sill (C_1) and range distance (a). The nugget effect is the combination of two components, namely: the sampling error and the error arising from variability on the scale immediately below that of measurement. Sill represents the semi-variance at which the variogram model equals the range distance, which is close to the sample variance of the data. Finally, the range distance is the limit of the spatial dependence between samples; thus, samples falling beyond the range distance exhibit no mutual spatial dependence (Isaaks and Srivastava, 1989).

The best model for fitting the experimental variograms, which was identified by cross-validation, was based on the coefficient of determination R^2 for the fitted data. With cross-validation, the experimental and estimated attribute values were used to calculate the root mean square error according to Hengl (2007):

$$\text{RMSE} = \left\{ \frac{1}{n} \sum_{i=1}^{n} \left[z(x_i) - \hat{z}(x_i) \right]^2 \right\}^{0,5} \quad (5)$$

where n is the number of values used for validation, $z(x_i)$ is the value of the property concerned at point i, and $\hat{z}(x_i)$ the estimated value at the same point. The lower the RMSE is, the greater is the accuracy of estimate. Semivariances were calculated and the models fitted to the experimental variograms by using the software GS+ version 9.0 (Gamma Design Software, 2008).

Please cite this article in press as: Bahia, A.S.R.S., et al., Iron oxides as proxies for characterizing anisotropy in soil CO_2 emission in sugarcane areas under green harvest. Agric. Ecosyst. Environ. (2014), http://dx.doi.org/10.1016/j.agee.2014.04.017

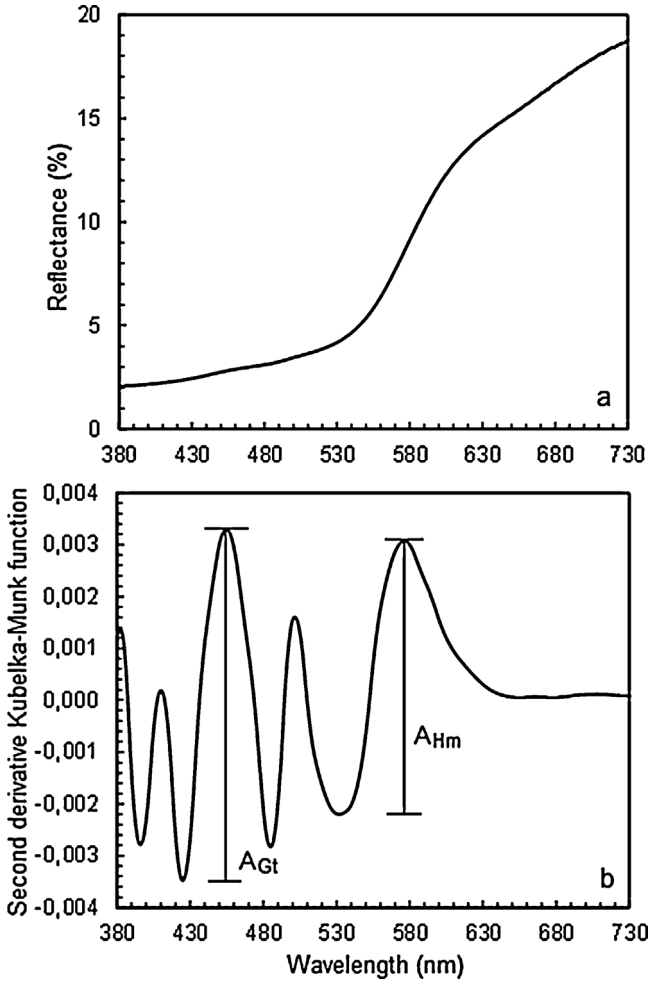

Fig. 2. (a) Diffuse reflectance spectrum and (b) second derivative of the Kubelka–Munk function with amplitudes of the spectral bands assigned to goethite (A_{Gt}) and hematite (A_{Hm}).

Multivariate statistics were calculated with Statistica v. 7.0 (StatSoft, Inc., Tulsa, OK, USA). Principal component analysis (PCA) was used to group variables with similar behavior to identify potential sources of variability. PCA is a multivariate technique that reduces the set of measured variables to a new set of unmeasured variables to assess the discriminant power of the original variables. Only those principal components with greater than unity eigenvalues were considered (Kaiser, 1958). A PC1 vs PC2 two-dimensional graph, known as a "biplot", allowed the soil property structure to be elucidated and the maximum variability of the properties as a whole to be assessed. The sampling direction effect was assessed via ANOVA of each principal component's score.

We performed a multiple linear regression analysis with isotropic and anisotropic spatial models to better expose the relationships between FCO_2 and soil properties. Regression curves were fitted by using the stepwise variable selection method, which identifies the best input variable subset for constructing a model. The method initially uses the whole set of variables and gradually discards the least significant. This process is repeated until all subset variables remaining are statistically relevant (i.e., until no further improvement is obtained or no additional variables can be discarded). The stepwise method assumes that some variables contribute negligibly to the response for the whole set (Demuth et al., 2008). In this work, we used FCO_2 as the dependent variable and all other soil properties as independent variables. The *F*-test significance level used to retain or discard variables was set at $p = 0.10$ and multiple linear regression calculations were done with SAS v. 9.0 (SAS Institute, Cary, NC, USA) software.

3. Results and discussion

3.1. Identification of anisotropy in soil properties

The mean values of the mineralogical attributes hematite (Hm), goethite (Gt), and iron oxides extracted by dithionite–citrate–bicarbonate (Fe_d), exhibited significant differences at the $p < 0.01$ level between directions in the four transects. As can be seen from Table 1, the smallest means of the mineralogical attributes were obtained in the 0° direction, which also exhibited the lowest CO_2 emission values (1.72 $\mu mol\, m^{-2}\, s^{-1}$). This is consistent with the previous findings of Panosso et al. (2012). These results provide the first evidence of a direct relationship between FCO_2 and mineralogical attributes. Based on the classification of Warrick and Nielsen (1980), spatial variability in Fe_d was low (CV < 12%) in all directions except 0°, where it was moderate (12% < CV < 24%). Spatial variability in Hm was moderate in the 0° and 90° directions, and low in the 45° and 135° directions, whereas that in Gt was high in all directions except 135°, where it was low (9.2%). These results indicate the presence of considerable variability in mineralogical attributes and justify using geostatistics to facilitate its spatial characterization (Camargo et al., 2013). The mean values and variation coefficients for the attributes soil CO_2 emission (FCO_2), free water porosity (FWP), temperature (T_s), moisture (M_s) and bulk density (D_s) were reported in a previous paper by Panosso et al. (2012).

Based on the geostatistical analysis performed, nearly all variables exhibited spatial dependence; thus, applying the two mathematical models to the variograms for the different directions in each transect revealed anisotropy in the target variables and especially, in the mineralogical attributes (Table 2, Fig. 3). In their study of a Brazilian Latosol, Souza et al. (2003) found chemical and grain size-related attributes to vary differently between grid directions (i.e., to exhibit anisotropy). Carvalho et al. (2002) examined spatial variability in soil chemical attributes and found it to be especially marked in the direction where the soil was plowed along the planting line. They concluded that soil management along that direction might have introduced chemical attribute anisotropy.

Heterogeneity is an intrinsic property of soil resulting from environmental influence on soil formation and minerals (Kämpf and Curi, 2000). Soil use and management can increase or decrease variability in physical, chemical and biological attributes (Souza et al., 2001). It can also alter the pedoenvironmental status of soil, particularly in areas where conventional tillage is replaced with no-tillage (Inda et al., 2013).

The spherical model proved better to fit the variograms for the attributes FCO_2, T_s, M_s (135°), FWP, D_s, Fe_d (isotropic, 0° and 135°), and Gt (isotropic, 0° and 45°), whereas the exponential model was more effective with M_s (isotropic, 0°, 45° and 90°), Fe_d (45° and 90°), Hm, and Gt (135°). Spherical and exponential models describe relatively irregular phenomena with a linear variogram close to the origin, the latter being a better choice for phenomena that are subject to especially erratic changes over small distances (Isaaks and Srivastava, 1989).

The spherical model is the most effective choice for typically examined soil properties, by virtue of its efficiently capturing abrupt spatial changes in soil variables (Cambardella et al., 1994; Vieira, 2000). Teixeira et al. (2011) used spherical models to fit FCO_2 variograms in the same type of soil; by exception, the exponential method proved better with soil density. Camargo et al. (2010) assessed spatial variability in physical attributes of an Ultisol on two (concave and convex) 100 m × 100 m sampling grids, and used

Please cite this article in press as: Bahia, A.S.R.S., et al., Iron oxides as proxies for characterizing anisotropy in soil CO_2 emission in sugarcane areas under green harvest. Agric. Ecosyst. Environ. (2014), http://dx.doi.org/10.1016/j.agee.2014.04.017

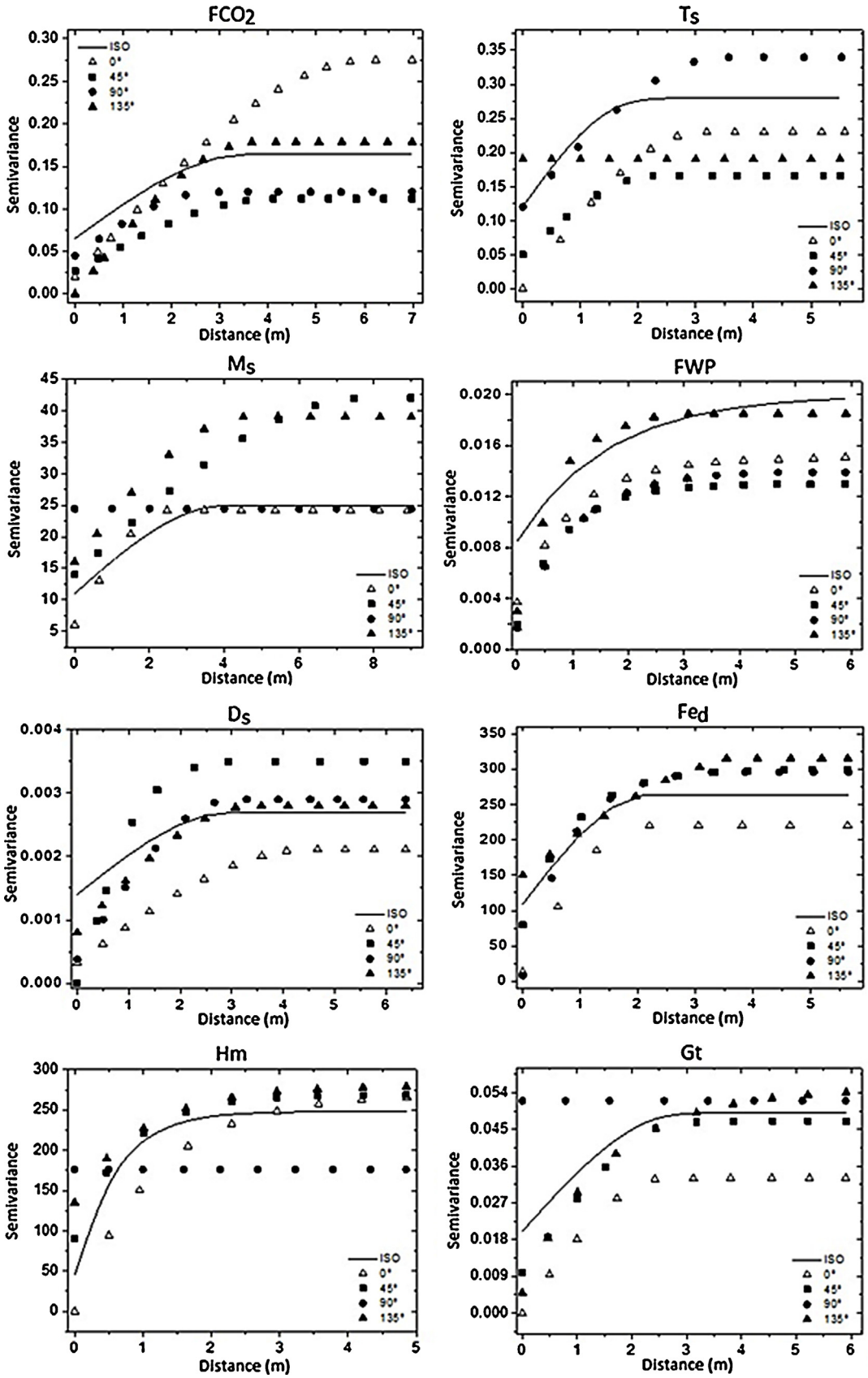

Fig. 3. Variograms of CO_2 emission and the other soil attributes in the different directions. FCO_2 = soil CO_2 emission; T_s = soil temperature; M_s = soil moisture; FWP = free water porosity; D_s = soil density; Fe_d = iron oxides extracted by dithionite–citrate–bicarbonate; Hm = hematite; Gt = goethite.

Please cite this article in press as: Bahia, A.S.R.S., et al., Iron oxides as proxies for characterizing anisotropy in soil CO_2 emission in sugarcane areas under green harvest. Agric. Ecosyst. Environ. (2014), http://dx.doi.org/10.1016/j.agee.2014.04.017

Table 1
Mean values of the soil attributes and coefficients of variation (CV) in different directions as determined in the 0.0–0.1 m layer.

Attributes	0°		45°		90°		135°	
	Mean	CV	Mean	CV	Mean	CV	Mean	CV
*FCO_2	1.72 b	32.1	2.42 a	41.1	2.29 ab	24.4	2.42 a	35.2
*T_s	26.24 a	1.6	25.78 a	1.6	25.96 a	2.8	25.96 a	2.4
*M_s	31.07 a	21.7	26.68 b	11.1	27.07 b	9.6	26.74 b	14.4
*FWP	9.34 b	68.5	16.75 a	27.2	16.84 a	21.5	17.03 a	29.2
*D_s	1.22 a	2.7	1.15 b	6.4	1.15 b	4.9	1.15 b	5.8
Fe_d	81.16 b	13.3	112.59 a	9.8	110.73 a	11.3	115.12 a	6.9
Hm	80.32 b	15.4	113.79 a	10.9	105.62 a	12.7	112.80 a	7.6
Gt	32.83 b	14.7	45.07 a	13.1	41.59 a	14.4	44.71 a	9.2

Values followed by the same letter were not significantly different as per Tukey's test at $p < 0.05$. $N = 89$; FCO_2 = soil CO_2 emission (mmol m^{-2} s^{-1}); T_s = soil temperature (°C); M_s = soil moisture (%); FWP = free water porosity (%); D_s = soil density (g cm^{-3}); Fe_d = iron oxides extracted by dithionite–citrate–bicarbonate (g kg^{-1}); Hm = hematite (g kg^{-1}); Gt = goethite (g kg^{-1}).

* Data described by Panosso et al. (2012).

spherical and exponential models to elucidate their potential relationship to the landscape.

The $C_0/(C_0 + C_1)$ ratio allows assessment of the degree of soil properties' spatial dependence to be assessed by Cambardella et al. (1994), such a dependence is strong if $C_0/(C_0 + C_1) < 0.25$, moderate if $0.25 < C_0/(C_0 + C_1) < 0.75$, and weak if $C_0/(C_0 + C_1) > 0.75$ (Table 2). Most of the target attributes exhibited moderate to strong spatial dependence. According to Cambardella et al. (1994) and Castrignanò et al. (2000), a strong spatial dependence of soil properties can be ascribed to such intrinsic factors, such as, source material, climate and landscape form. On the other hand, a weak spatial dependence reflects chaotic variability of attributes and suggests intensifying the sampling in order to expose a potentially greater spatial continuity (Cambardella et al., 1994). In this work, the variables T_s (135°), FWP (90°), Hm (90°) and Gt (90°) exhibited a pure nugget effect (PNE), i.e., no definite spatial variability structure at for the sampling scale used. PNE occurs when the semi-variance of a variable at a given distance h is constant and the variable

Table 2
Model types used to fit the variograms for the soil attributes and fitting parameters in the different directions.

		Model	C_0	$C_0 + C_1$	$C_0/(C_0 + C_1)$	a	R^2	RMSE	RI
	ISO	Spher.	0.06	0.16	0.39	3.60	0.99	0.13	–
	0°	Spher.	0.02	0.27	0.07	6.18	0.91	0.10	23.08
FCO_2	45°	Spher.	0.02	0.11	0.24	4.12	0.84	0.13	0.00
	90°	Spher.	0.04	0.12	0.37	2.80	0.75	0.12	7.69
	135°	Spher.	1.00E − 07	0.18	5.60E − 07	3.75	0.96	0.13	0.00
	ISO	Spher.	0.12	0.28	0.43	2.00	0.96	0.06	–
	0°	Spher.	1.00E − 07	0.23	4.35E − 07	3.10	0.95	0.09	−50.00
T_s	45°	Spher.	0.05	0.17	0.30	2.30	0.86	0.10	−66.67
	90°	Spher.	0.12	0.34	0.35	3.50	0.93	0.12	−100.00
	135°	PNE	0.19	0.19	1.00	–	–	–	–
	ISO	Exp.	0.01	0.02	0.43	4.90	0.95	2.78	–
	0°	Exp.	3.70E − 03	0.02	0.25	3.00	0.69	0.82	70.50
M_s	45°	Exp.	2.00E − 03	0.01	0.15	2.50	0.76	0.62	77.70
	90°	Exp.	1.70E − 03	0.01	0.12	3.00	0.83	0.65	76.62
	135°	Spher.	3.70E − 03	0.02	0.16	1.50	0.79	0.89	67.99
	ISO	Spher.	11.00	25.00	0.44	4.00	0.81	1.11	–
	0°	Spher.	6.00	24.20	0.25	2.50	0.96	0.94	15.32
FWP	45°	Spher.	14.00	42.00	0.33	7.80	0.98	1.01	9.01
	90°	PNE	24.44	24.44	1.00	–	–	–	–
	135°	Spher.	16.00	39.00	0.41	4.60	0.94	1.09	1.80
	ISO	Spher.	1.40E − 03	2.70E − 03	0.52	3.00	0.90	0.05	–
	0°	Spher.	3.20E − 04	2.11E − 03	0.15	4.50	0.83	0.01	80.00
D_s	45°	Spher.	1.00E − 07	3.50E − 03	2.86E − 05	2.00	0.84	0.01	80.00
	90°	Spher.	3.80E − 04	2.90E − 03	0.13	3.00	0.92	0.01	80.00
	135°	Spher.	8.00E − 04	2.80E − 03	0.29	3.40	0.90	0.01	80.00
	ISO	Spher.	109.00	264.00	0.41	2.20	0.82	3.93	–
	0°	Spher.	13.00	220.00	0.06	2.00	0.93	3.81	3.05
Fe_d	45°	Exp.	80.00	300.00	0.27	2.60	0.85	2.92	25.70
	90°	Exp.	8.00	300.00	0.03	2.35	0.99	2.23	43.26
	135°	Spher.	150.00	315.00	0.48	4.00	0.72	2.18	44.53
	ISO	Exp	45.00	248.00	0.18	1.60	0.93	4.82	–
	0°	Exp	0.00	270.00	0.00	3.50	0.86	4.78	0.83
Hm	45°	Exp	90.00	269.00	0.33	2.30	0.81	3.04	36.93
	90°	PNE	176.10	176.10	1.00	–	–	–	–
	135°	Exp	135.00	280.00	0.48	3.00	0.72	2.48	48.55
	ISO	Spher.	0.02	0.05	0.41	2.90	0.84	4.41	–
	0°	Spher.	0.00	0.03	0.00	2.60	0.92	1.78	59.64
Gt	45°	Spher.	0.01	0.05	0.21	3.00	0.80	1.71	61.22
	90°	PNE	0.05	0.05	1.00	–	–	–	–
	135°	Exp.	0.01	0.06	0.17	4.50	0.58	1.05	76.19

C_0 = nugget effect; $C_0 + C_1$ = sill; $C_0/(C_0 + C_1)$ = degree of spatial dependence; a = range distance (m); RMSE = mean square root error; RI = relative improvement (%); FCO_2 = soil CO_2 emission (mmol m^{-2} s^{-1}); T_s = soil temperature (°C); M_s = soil moisture (%); FWP = free water porosity (%); D_s = soil density (g cm^{-3}); Fe_d = iron oxides extracted by dithionite-citrate-bicarbonate (g kg^{-1}); Hm = hematite (g kg^{-1}); Gt = goethite (g kg^{-1}); Exp. = exponential; Spher. = spherical; PNE = pure nugget effect.

Please cite this article in press as: Bahia, A.S.R.S., et al., Iron oxides as proxies for characterizing anisotropy in soil CO_2 emission in sugarcane areas under green harvest. Agric. Ecosyst. Environ. (2014), http://dx.doi.org/10.1016/j.agee.2014.04.017

Table 3
Correlation coefficients between soil attributes and the first two principal components, and results of the analysis of variance and multiple comparison test of the variables in different directions.

Attributes	Principal component			
	PC1		PC2	
	Correlation	Ranking	Correlation	Ranking
FCO_2	−0.73*	11.9	0.37	9.7
D_s	0.58*	7.6	−0.35	8.6
T_s	0.45	4.6	−0.38	10.1
M_s	0.75*	12.8	−0.37	9.9
FWP	−0.87*	16.9	0.35	8.8
Fe_d	−0.82*	15.1	−0.52*	19.0
Hm	−0.86*	16.8	−0.45	14.2
Gt	−0.80*	14.3	−0.53*	19.7
Eigenvalue	4.5		1.4	
Variance explained (%)	55.7		17.7	
Cumulative variance (%)	55.7		73.4	

$N = 89$; * Correlations were used for interpretation (>0.50); FCO_2 = soil CO_2 emission (mmol m^{-2} s^{-1}); D_s = soil density (g cm^{-3}); T_s = soil temperature (°C); M_s = soil moisture (%); FWP = free water porosity (%); Fe_d = iron oxides extracted by dithionite-citrate-bicarbonate (g kg^{-1}); Hm = hematite (g kg^{-1}); Gt = goethite (g kg^{-1}).

concerned is therefore space-independent. One plausible explanation for this effect's presence in the variability of a soil attribute is that the attribute's range distance is smaller than the smallest distance between samples (0.50 m in this work), in which case, it will exhibit a totally random distribution (Cambardella et al., 1994).

The above-described results testify to the importance of using various sampling strategies to facilitate spatial variability capture at different scales, thereby identifying potential anisotropy in the target properties. Regular (La Scala et al., 2000; Herbst et al., 2009, 2012), irregular (Teixeira et al., 2011) and dense irregular sampling schemes (Herbst et al., 2009) frequently allow for successful spatial variability capture in soil properties. By contrast, star-shaped sampling designs (Panosso et al., 2012), which was used in this work, are more suitable for the joint capture of variability at different scales or in different directions and hence, for identifying anisotropy.

The range distances for the fitted models differed markedly between directions, further confirming the need to carefully assess anisotropy in soil phenomena and processes (Table 2). The greatest range distances were those for FCO_2 in the 0° direction and FWP in the 45° direction. Since the variables exhibited a nugget effect, their range distances were possibly smaller than the smallest sampling distance used (0.50 m). Consequently, the attributes T_s in the 135° direction, and FWP, Hm and Gt, all in the 90° direction, exhibited decreased variability and therefore, in those directions, reflected smaller range distances. Also, the greatest and smallest range distance for FCO_2 (6.18 and 2.80 m, respectively) coincided with the greatest (3.50 m) and smallest value (PNE) for Hm in the 0° and 90° direction, respectively. This suggests a potential relationship between the spatial variability patterns for these soil properties.

This study's range distances for FCO_2 are similar to those reported by Kosugi et al. (2007) for forest areas, where bands were detected from 4.40 to 24.70 m in an isotropic 50 m × 50 m sampling grid. Oliveira Jr. et al. (2011) reported range distances exceeding ours for Hm (77.70 m) and Gt (28.90 m), as estimated by X-ray diffraction, in a 12.88 ha sampling area with points 1–15 m apart.

The root mean square error (RMSE) provides information about the accuracy of the model for each variable (Chirico et al., 2007). The lower the RMSE is, the lower the dispersion of data around the model will be. The relative improvement (RI in Table 2) is the performance ratio of the interpolators used to compare isotropic and anisotropic variograms. As revealed by comparing isotropic and anisotropic variograms, Gt in the 135° direction was the individual mineralogical attribute determined with the lowest accuracy; using anisotropic variograms improved the accuracy by 76.19% (Table 2). Indeed, all variables except T_s benefited from the use of anisotropic variograms. This testifies to the potential of anisotropic variograms for improving accuracy in data acquisition and describing spatial distribution in soil properties.

3.2. Principal component analysis

Table 3 shows the results of the principal component analysis (PCA) used to assess the discriminant power of the target soil properties. As can be seen from Table 3, the first two PCs jointly accounted for 73.4% of variability in the data. In a similar study, Panosso et al. (2012) found that 66.8% of the total variance was explained by three PCs, the first relating essentially to soil physical attributes. In this work, PC1 correlated mainly with physical attributes (D_s, M_s and FWP), which are largely associated with gas transfer and O_2 and CO_2 soil-atmosphere balance (Fang and Moncrief, 1999). Additionally, PC1 correlated with iron oxides (Fe_d, Hm and Gt), which are closely related to aggregation of soil mineral particles (Muggler et al., 1999; Inda et al., 2007; Inda et al., 2013). By contrast, PC2 correlated with the mineralogical attributes Gt and Fe_d.

A two-dimensional plot of the two PCs revealed clustering along the planting line (0°). As can be seen from Fig. 4, PC1 discriminated between diagnostic attributes (Fe_d, Hm and Gt) and secondary attributes (D_s, M_s and T_s), which fell separately in the biplot. This result affirms the relationship between these attributes and the spatial variability pattern, thereby confirming the assumption that pedogenic variables are related to spatial variability in soil physical attributes (Camargo et al., 2010; Camargo et al., 2013).

Ghidin et al. (2006) found increased macroporosity, total porosity, and decreased soil density influences Hm, Gt and gibbsite content in toposequences from southern Brazil, thereby providing evidence for a dependence of these minerals on soil relief and physical properties. The variables D_s, M_s and T_s enabled discrimination: this group fell to the right of PC1 (positive correlation). On the other hand, FCO_2, FWP, Fe_d, Hm and Gt fell to the left of PC1 (negative correlation) and were thus antagonists to the 0° direction points. The variables PLA (−0.87), Hm (−0.86), Fe_d (−0.82), Gt (−0.80), M_s (0.75), FCO_2 (−0.73) and D_s (0.58), exhibited the greatest discriminating power in PC1, whereas Gt (−0.53) and Fe_d (−0.52) were the only discriminant variables for PC2. PC1 attributes had a substantially increased discriminant power relative to those previously studied by Panosso et al. (2012). This strengthens the notion that mineralogical attributes hold a high potential for characterizing spatial variability in FCO_2.

Please cite this article in press as: Bahia, A.S.R.S., et al., Iron oxides as proxies for characterizing anisotropy in soil CO_2 emission in sugarcane areas under green harvest. Agric. Ecosyst. Environ. (2014), http://dx.doi.org/10.1016/j.agee.2014.04.017

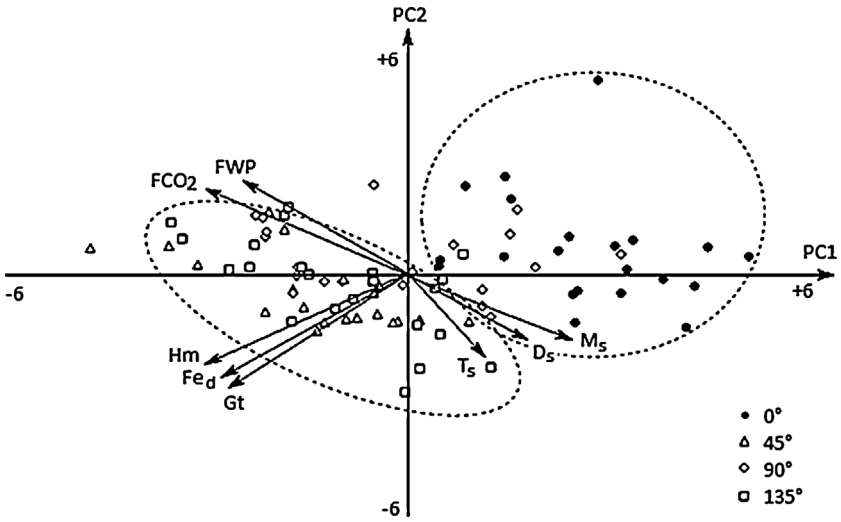

Fig. 4. Two-dimensional plot of the first two principal components (biplot). FCO_2 = soil CO_2 emission; FWP = free water porosity; T_s = soil temperature; D_s = soil density; M_s = soil moisture; Fe_d = iron oxides extracted by dithionite-citrate-bicarbonate; Hm = hematite; Gt = goethite.

We found the target soil properties' spatial variability to depend on particular grid sampling directions used. Thus, there were anisotropic groups consisting of points falling on a given sampling direction. Those management practices performed in the planting line direction of the planting line (soil preparation and crop harvesting, mainly) influenced attribute behavior in that direction (0°) and reflected in separation of the corresponding points in the biplot (Fig. 4). Also, the other points tended to distribute in the same region (left side). *T*; this was particularly so in the 45° and 135° directions, which coincided with those of soil preparation for fallow. The attributes falling on that side (FCO_2, FWP, Fe_d, Hm and Gt) were jointly designated the 45° and 135° anisotropic groups. This result may reflect an anthropic effect on the spatial distribution of soil properties – FCO_2 include – in sugarcane-cropped areas, since such directions coincide with those of stubble removal for fallow. According to Inda et al. (2013), direct planting on maize, oat and bean stubble alters pedoenvironmental conditions and as a result, affects dissolution of iron oxides as a result, which is consistent with the assumption that soil preparation can influence soil mineralogy, and hence, respiration.

Similar effects were previously observed in a multivariate analysis involving a larger number of variables (viz., macroporosity, total pore volume, clay content, pH, cation exchange capacity, carbon stock, FCO_2, T_s and FWP) performed by Panosso et al. (2012). Their study found FCO_2 variability to be accounted for by changes in FWP. The results of our study found, by using the simpler approach of Geostatistics in combination with PCA, that FCO_2 anisotropy is also dependent on the mineralogical attributes Hm, Gt and Fe_d because the content in iron oxides is closely related to soil aggregation (Muggler et al., 1999; Inda et al., 2007, 2013).

3.3. Multiple linear regression analysis

Multiple linear regression analysis was used to identify the specific attributes best explaining FCO_2 spatial variability on the sampling grid (isotropic model) and its different directions (anisotropic models) (see Table 4). As in previous work (Panosso et al., 2012), the variable FWP was selected in almost all variants, whether isotropic or anisotropic. In fact, FWP is assumed to have a marked influence on soil CO_2 emission in green-harvested sugarcane areas. Soil respiration results from the production and transfer of CO_2 from soil to the atmosphere (Luo and Zhou, 2006) particularly through the breakdown of organic compounds by microorganisms. Therefore, FCO_2 is also affected by variables associated with these processes. FWP, which is a measure of the volume of pores not filled with water, has a direct effect on gas transport in soil (both on the oxygen input required for aerobic microbial activity and on the CO_2 output as a microbial activity byproduct). The positive correlation between FWP and FCO_2 may be associated with the negative effect of soil moisture on gas diffusion (Davidson et al., 2000; Schwendenmann et al., 2003; Kosugi et al., 2007). When soil moisture is decreased by an increase in soil temperature (Luo and Zhou, 2006), the volume of air-filled pore space increases and so does microbial activity. This facilitates CO_2 release into the atmosphere (Fang and Moncrief, 1999; Nobel, 2005). Organic matter is believed to be the primary energy source used by microorganisms, hence its positive correlation with soil CO_2 emission (Luo and Zhou, 2006).

In recent work, Panosso et al. (2011) used multiple linear regression analysis to model CO_2 emission in sugarcane areas under either green or slash-and-burn harvest, and found FWP to be selected by both methods. FWP, in fact, explained 18% of the soil respiration

Table 4
Multiple linear regression models for soil CO_2 emission in the sampling grid (isotropic) and in different directions (anisotropic).

Variável	R^2	*p*
Isotropic		
$FCO_2 = 4.07 - 2.58FWP$	0.48	<0.001
$FCO_2 = 4.07 - 2.58FWP + 0.08D_S$	0.51	0.032
Anisotropic		
0°		
$FCO_2 = 1.24 + 0.05FWP$	0.34	0.005
45°		
$FCO_2 = -3.31 + 0.13FWP$	0.58	<0.001
$FCO_2 = -3.31 + 0.13FWP + 0.03Hm$	0.71	0.015
90°		
$FCO_2 = -0.52 + 0.07FWP$	0.38	0.003
$FCO_2 = -0.52 + 0.07FWP + 0.01Fe_d$	0.46	0.126
135°		
$FCO_2 = 16.32 - 0.12M_S$	0.54	<0.001
$FCO_2 = 16.32 - 0.12M_S + 0.41T_S$	0.61	0.115

R^2 = Coefficient of determination; FCO_2 = soil CO_2 emission (mmol m^{-2} s^{-1}); FWP = free water porosity (%); D_s = soil density (g cm^{-3}); Hm = hematite (g kg^{-1}); Fe_d = iron oxides extracted by dithionite–citrate–bicarbonate (g kg^{-1}); M_s = soil moisture (%); T_s = soil temperature (°C).

Please cite this article in press as: Bahia, A.S.R.S., et al., Iron oxides as proxies for characterizing anisotropy in soil CO_2 emission in sugarcane areas under green harvest. Agric. Ecosyst. Environ. (2014), http://dx.doi.org/10.1016/j.agee.2014.04.017

variability in the area under green harvest. Linn and Doran (1984) assessed the effect that the degree of pore filling with water had on soil respiration and found the effect peaked at about 60% pore filling and a density of 1.40 g cm^{-3}. These conditions are extremely different from those of our work, where pore filling amounted to only 37% on average.

Other soil properties, including T_s, Fe_d, and Hm, were among the specific attributes influencing soil respiration selected by the model. Iron oxides play a crucial role in the physical protection and colloid stability of organic matter in tropical and subtropical soils (Inda et al., 2007); therefore, together with T_s, they influence FCO_2. The variable FWP was the first to be selected by the isotropic model, where it explained 48% of the variability in FCO_2. Incorporating D_s increased the coefficient of determination, R^2, to 51%. As can be seen from Table 4, D_s and FWP were directly and inversely related, respectively, to FCO_2. Soil temperature and moisture (Epron et al., 2006; Ryu et al., 2009), and density and porosity (Saiz et al., 2006), have also been cited as influential factors for spatial variability in FCO_2. These soil properties are closely related to FCO_2; in fact, they are primarily responsible for soil oxygenation and atmospheric CO_2 transfer (Fang and Moncrief, 1999; Xu and Qi, 2001; Saiz et al., 2006; Panosso et al., 2012).

As previously found by Panosso et al. (2012), R^2 changed with sampling direction and peaked at 71% in the 45° direction. Only FWP was selected for the 0° direction, where it accounted for a mere 34% of FCO_2 variability (Table 4). The model for the 45° direction included the variables FWP and Hm, which jointly explained 71% of the variability in FCO_2. The positive sign of the Hm parameter may have been a result of iron oxides influencing FCO_2 (La Scala et al., 2000). Iron oxides are aggregating agents associated with mineral particles (Muggler et al., 1999; Inda et al., 2007, 2013) and soil structure conditioning. Thus, in addition to protecting organic matter fractions from microorganism degradation, they facilitate soil aggregation and, as a result, boost FCO_2. Consequently, increasing aggregation makes soil more porous, thereby increasing empty spaces and, as per Fick's Law, facilitating the release of soil gases into the atmosphere (Ghildyal, 1987; Nazaroff, 1992).

In this work, FCO_2 results identical to those previously reported by Panosso et al. (2012) were obtained in a simpler manner from the mineralogical attributes Gt, Hm and Fe_d. They found that 74% of spatial variability in FCO_2 was explained by FWP and sand content. Although their R^2 values were slightly higher than ours, in this study FWP in combination with a single additional mineralogical attribute accounted for 71% of FCO_2 variability. In addition, the methodology used in this study to estimate Hm and Gt is simpler and more expeditious than conventional methods for soil physical attributes. The 90° direction model included the variables FWP and Fe_d, in this sequence, and in combination, accounted for 46% of FCO_2 variability. The attribute Fe_d had a positive estimated parameter in that direction (i.e., Fe_d was directly related to the variability in FCO_2), which testifies to the complex relationship of soil respiration to mineralogical (La Scala et al., 2000) and chemical attributes (Ekblad and Nordgren, 2002; Savin et al., 2001).

Finally, the model for the 135° direction only included the variables M_s and T_s, which jointly accounted for 61% of the FCO_2 variability. The estimated parameter for moisture in this direction was negative, whereas that for temperature was positive. Therefore, M_s was inversely related to soil respiration (Davidson et al., 2000; Schwendenmann et al., 2003; Luo and Zhou, 2006; Kosugi et al., 2007); by contrast, T_s was positively related to FCO_2 (Nobel, 2005; Luo and Zhou, 2006). These attributes are the two main factors associated with soil microbial activity influencing FCO_2 (Ryu et al., 2009). According to Luo and Zhou (2006), organic matter decomposition is governed by various factors besides the oxygen availability, including M_s and T_s. According to these authors, temperature indirectly influences soil respiration through soil moisture, which in turn has a negative effect on FCO_2. Also, according to Nobel (2005), gas diffusion in soil increases with temperature and moisture, up to a certain soil water volume that is required to diffusion occur. Therefore, soil with high moisture content can hinder emission of CO_2 into the atmosphere.

In this work, spatial variability in soil CO_2 emission was found to be related to spatial changes in hematite, goethite and iron oxides extracted by dithionite–citrate–bicarbonate. This supports the assumption that mineralogical attributes influence soil respiration in plant-covered areas and indicates the potential of diffuse reflectance spectroscopy for mapping FCO_2 with Geostatistical techniques. The FCO_2 continues to be characterized on small sampling grids because CO_2 emission readings are subject to variation arising from temporal soil temperature changes. This shortcoming inhibits accurate mapping of large agricultural areas. Using DRS to facilitate characterization of FCO_2 influencing attributes is an effective choice because it affords direct, simple, and inexpensive measurements, which are not restricted by sampling time. Consequently, this methodology is an effective choice for mapping large areas, making informed decisions on sustainable agricultural practices, and identifying management systems and areas with an increased potential for soil carbon storage.

4. Conclusions

The soil properties examined in this study were found to be spatially dependent and to exhibit well-defined anisotropy (particularly in the mineralogical attributes hematite, goethite and iron oxides extracted by dithionite–citrate–bicarbonate). Our results indicate that soil preparation and management practices in mechanically harvested sugarcane areas affect various inherent soil formation factors, such as physical and mineralogical soil properties, which in turn influence CO_2 soil emissions. The proposed methodology provides a new, effective DRS-based tool for the simple, accurate, indirect quantitation of iron oxides, which are useful to identify anisotropy in soil CO_2 emission in green-harvested sugarcane areas. In addition, our methodology can be useful towards FCO_2 mapping in large areas with a view to develop greenhouse gas emission inventories for agricultural soils.

Acknowledgments

We are grateful to the Fundação de Amparo à Pesquisa do Estado de São Paulo (FAPESP) and Conselho Nacional de Desenvolvimento Científico e Tecnológico (CNPq) for the financial support and São Martinho mill for the facilities and area available to our study.

References

Allaire, S.E., Lange, S.F., Lafond, J.A., Pelletier, B., Cambouris, A.N., Dutilleul, P., 2012. Multiscale spatial variability of CO_2 emissions and correlations with physic-chemical soil properties. Geoderma 170, 251–260.
Andreae, M.O., Crutzen, P.J., 1997. Atmospheric aerosols: biogeochemical sources and role in atmospheric chemistry. Science 276, 1052–1058.
Barrón, V., Mello, J.W.V., Torrent, J., 2000. Caracterização de óxidos de ferro em solos por Espectroscopia de Reflectância Difusa. In: Novais, R.F., Alvarez, V.H., Schaefer, C.E.G.R. (Eds.), Tópicos em Ciência do Solo, Viçosa. Sociedade Brasileira de Ciência do Solo, Viçosa, MG, Brazil, pp. 139–162.
Benbi, D.K., Brar, J.S., 2009. A 25-year record of carbon sequestration and soil properties in intensive agriculture. Agron. Sustainable Dev. 29, 257–265.
Boeckx, P., Nieuland, K.V., Cleemput, O.V., 2011. Short-term effect of tillage intensity on N_2O and CO_2 emissions. Agron. Sustainable Dev. 31, 453–461.
Brito, L.F., Marques Jr., J., Pereira, G.T., La Scala, N., 2010. Spatial variability of soil CO_2 emission in different topographic positions. Bragantia 69, 19–27.
Camargo, L.A., Marques Jr., J., Pereira, G.T., 2010. Spatial variability of physical attributes of an alfisol under different hillslope curvatures. Rev. Bras. Cienc. Solo 34, 617–630.
Camargo, L.A., Marques Jr., J., Pereira, G.T., Alleoni, L.R.F., 2013. Spatial correlation between the composition of the clay fraction and contents of available phosphorus of an Oxisol at hillslope scale. Catena 100, 100–106.

Please cite this article in press as: Bahia, A.S.R.S., et al., Iron oxides as proxies for characterizing anisotropy in soil CO_2 emission in sugarcane areas under green harvest. Agric. Ecosyst. Environ. (2014), http://dx.doi.org/10.1016/j.agee.2014.04.017

Camargo, O.A., Moniz, A.C., Jorge, J.A., Valadares, L.M.A.S., 1986. Métodos de análise química, mineralógica e física dos solos do Instituto Agronômico de Campinas. Instituto Agronômico, Campinas, pp. 96.
Cambardella, C.A., Moorman, T.B., Novak, J.M., Parkin, T.B., Karlen, D.L., Turco, R.F., Konopka, A.E., 1994. Field-scale variability of soil properties in central Iowa soils. Soil Sci. Soc. Am. J. 58, 1501–1511.
Carvalho, J.R.P., Silveira, P.M., Vieira, S.R., 2002. Geoestatística na determinação da variabilidade espacial de características químicas do solo sob diferentes preparos. Pesq. Agropec. Bras. 37, 1151–1159.
Castrignanò, A., Giugliarini, L., Risaliti, R., Martinelli, N., 2000. Study of spatial relationships among some soil physicochemical properties of a field in central Italy using multivariate geostatistics. Geoderma 97, 39–60.
Cerri, C.C., Maia, S.M.F., Galdos, M.V., Cerri, C.E.P., Feigl, B.J., Bernoux, M., 2009. Brazilian greenhouse gas emissions: the importance of agriculture and livestock. Sci. Agric. 66, 831–843.
Cerri, C.E.P., Sparovek, G., Bernoux, M., Easterling, W.E., Melillo, J.M., Cerri, C.C., 2007. Tropical agriculture and global warming: impacts and mitigation options. Sci. Agric. 64, 83–99.
Chilès, J.P., Delfiner, P., 1999. Geostatistics: Modeling Spatial. John Wiley & Sons Inc, New York, NY.
Chirico, G.B., Medina, H., Romano, N., 2007. Uncertainty in predicting soil hydraulic properties at the hillslope scale with indirect methods. J. Hydrol. 334, 405–422.
Dasselaar, A.V.P.V., Corré, W.J., Priemé, A., Klemedtsson, Å.K., Weslien, P., Stein, A., Klemedtsson, L., Oenema, O., 1998. Spatial variability of methane, nitrous oxide and carbon dioxide emissions from drained grassland. Soil Sci. Soc. Am. J. 62, 810–817.
Davidson, E.A., Verchot, L.V., Cattânio, J.H., Ackerman, I.L., Carvalho, J.E.M., 2000. Effects of soil water content on soil respiration in forests and cattle pastures of eastern Amazonia. Biogeochemistry 48, 53–69.
De Figueiredo, E.B., La Scala, N., 2011. Greenhouse gas balance due to the conversion of sugarcane areas from burned to green harvest in Brazil. Agric. Ecosyst. Environ. 141, 77–85.
Demattê, J.A.M., Sousa, A.A., Alves, M.C., Nanni, M.R., Fiorio, P.R., Campos, R.C., 2006. Determining soil water status and other soil characteristics by spectral proximal sensing. Geoderma 135, 179–195.
Demuth, R., Gräsel, C., Parchmann, I., Ralle, B., 2008. Chemie im Kontext–Von der Innovation zur nachhaltigen Verbreitung eines Unterrichtskonzepts. Waxmann, Münster, Berlin.
Deutsch, C.V., Journel, A.G., 1998. GSLIB: Geostatistical Software Library and User's Guide, second ed. Oxford University Press, New York, NY.
Ekblad, A., Nordgren, A., 2002. Is growth of soil microorganisms in boreal forests limited by carbon or nitrogen availability? Plant Soil 242, 115–122.
EMBRAPA—Empresa Brasileira de Pesquisa Agropecuária, 1997. Centro Nacional de Pesquisa de Solos. Manual de métodos de análise de solo, second.ed. Ministério da Agricultura e do Abastecimento/EMBRAPA-CNPS, Brasília.
Epron, D., Bosc, A., Bonal, D., Freycon, V., 2006. Spatial variation of soil respiration across a topographic gradient in a tropical rain forest in French Guiana. J. Trop. Ecol. 22, 565–574.
Fang, C., Moncrief, J.B., 1999. A model for soil CO_2 production and transport. 1: Model development. Agric. For. Meteorol. 95, 225–236.
FAPESP—Fundação de Amparo à Pesquisa do Estado de São Paulo, 2008. Contribuições da pesquisa paulista para o conhecimento sobre mudanças climáticas. FAPESP—Fundação de Amparo à Pesquisa do Estado de São Paulo, São Paulo.
Gamma Design Software, 2008. GS+Geostatistics for the Enviromental Sciences, Version 9.0. Gamma Design Software, USA.
Ghidin, A.A., Melo, V.F., Lima, V.C., Lima, J.M.J.C., 2006. Toposseqüências de Latossolos originados de rochas basálticas no Paraná II–Relação entre mineralogia da fração argila e propriedades físicas dos solos. Rev. Bras. Cienc. Solo 30, 293–306.
Ghildyal, B., 1987. Soil Physics. Halsted Press, New Delhi.
Guerra, P.A.G., 1988. Geoestatística Operacional. Departamento Nacional de Produção Mineral, Brasília.
Hengl, T., 2007. A Practical Guide to Geostatistical Mapping of Environmental Variables. Office for Official Publications of the European Communities, Luxembourg, 146p.
Herbst, M., Bornemann, L., Graf, A., 2012. A geostatistical approach to the field-scale pattern of heterotrophic soil CO_2 emission using covariates. Biogeochemistry 111, 377–392.
Herbst, M., Prolingheuer, N., Graf, A., Huisman, J.A., Weihrmüller, L., Vandeborght, J., 2009. Characterization and understanding of bare soil respiration spatial variability at plot scale. Vadose Zone J. 8, 762–771.
Inda, A.V., Bayer, C., Conceição, P.C., Boeni, M., Salton, J.C., Tonin, A.T., 2007. Variáveis relacionadas à estabilidade de complexos organominerais em solos tropicais e subtropicais brasileiros. Rev. Ci. Rural 37, 1301–1307.
Inda, A.V., Torrent, J., Barrón, V., Bayer, C., Fink, J.R., 2013. Iron oxides dynamics in a subtropical Brazilian Paleudult under long-term no-tillage management. Sci. Agric. 70, 48–54.
Isaaks, E.H., Srivastava, R.M., 1989. An Introduction to Applied Geostatistics. Oxford University Press, New York, NY.
Janik, L.J., Merry, R.H., Skjemstad, J.O., 1998. Can mid infrared diffuse reflectance analysis replace soil extractions? Anim. Prod. Sci. 38, 681–696.
Journel, A.G., Huijbregts, C.J., 1978. Mining Geostatistics. Academic Press, London.
Kaiser, H.F., 1958. The varimax criterion for analytic rotation in factor analysis. Psychometrika 23, 178–200.
Kämpf, N., Curi, N., 2000. Óxidos de ferro: indicadores de ambientes pedogênicos. In: Novais, R.F., Alvarez, V.V.H., Schaefer, C.E.G.R. (Eds.), Tópicos em Ciência do Solo. Sociedade Brasileira de Ciência do Solo, Viçosa, MG, pp. 107–138.
Konda, R., Ohta, S., Ishizuka, S., Aria, S., Ansori, S., Tanaka, N., Hardjono, A., 2010. Seasonal changes in the spatial structures of N_2O CO_2, and CH_4 fluxes from *Acacia mangium* plantation soils in Indonesia. Soil Biol. Biochem. 42, 1512–1522.
Kosmas, C.S., Curi, N., Bryant, R.B., 1984. Characterization of iron oxide minerals by second-derivative visible spectroscopy. Soil Sci. Soc. Am. J. 48, 401–405.
Kosugi, Y., Mitani, T., Ltoh, M., Noguchi, S., Tani, M., Matsuo, N., Takanashi, S., Ohkubo, S., Nik, A.R., 2007. Spatial and temporal variation in soil respiration in a Southeast Asian tropical rainforest. Agric. For. Meteorol. 147, 35–47.
Kubelka, P., Munk, F., 1931. Ein beitrag zur optic der farbanstriche. Z. Tech. Phys. 12, 593–620.
La Scala, N., Marques Jr., J., Pereira, G.T., Corá, J.E., 2000. Carbon dioxide emission related to chemical properties of a tropical bare soil. Soil Biol. Biochem. 32, 1469–1473.
La Scala, N., Panosso, A.R., Pereira, G.T., Gonzalez, A.P., Miranda, J.G.V., 2009. Fractal dimension and anisotropy of soil CO_2 emission in an agricultural field during fallow. Int. Agrophys. 23, 353–358.
Linn, D.M., Doran, J.W., 1984. Effect of water-filled pore space on carbon dioxide and nitrous oxide production in tilled and non-tilled soils. Soil Sci. Soc. Am. J. 48, 1267–1272.
Luo, Y., Zhou, X., 2006. Soil Respiration and the Environment. Academic Press, USA.
Martin, J.G., Bolstad, P.V., 2009. Variation of soil respiration at three spatial scales: components within measurements intra-site variation and patterns on the landscape. Soil Biol. Biochem. 41, 530–543.
Mehra, O.P., Jackson, M.L., 1960. Iron oxide removal from soils and clays by a dithionite-citrate system buffered with sodium bicarbonate. In: Swineford, A.D.A. (Ed.), National Conference on Clays and Clay Minerals. Washington, pp. 317–342.
Muggler, C.C., Van Griethuysen, C., Buurman, P., Pape, T., 1999. Aggregation, organic matter, and iron oxide morphology in Oxisoil from Minas Gerais. Brazil. Soil Sci. 164, 759–770.
Nazaroff, W.W., 1992. Radon transport from soil to air. Rev. Geophys. (Washington).
Nobel, P.S., 2005. Physiochemical and Environmental Plant Physiology. Elsevier Academic Press, Amsterdam.
Oliveira Jr., J.C., Souza, L.C.P., Melo, V.F., Rocha, H.O., 2011. Variabilidade espacial de atributos mineralógicos de solos da formação Guabirotuba, Curitiba (PR). Rev. Bras. Cienc. Solo 35, 1481–1490.
Panosso, A.R., Marques Jr., J., Milori, D.M.B.P., Ferraudo, A.S., Barbieri, D.M., Pereira, G.T., La Scala, N., 2011. Soil CO_2 emission and its relation to soil properties in sugarcane areas under Slash-and-burn and Green harvest. Soil Tillage Res. 111, 190–196.
Panosso, A.R., Perillo, L.I., Ferraudo, A.S., Pereira, G.T., Miranda, J.G.V., La Scala, N., 2012. Fractal dimension and anisotropy of soil CO_2 emission in a mechanically harvested sugarcane production área. Soil Tillage Res. 124, 8–16.
Ryu, S., Concilio, A., Chen, J., North, M., Ma, S., 2009. Prescribed burning and mechanical thinning effects on belowground conditions and soil respiration in a mixed-conifer forest, CA. For. Ecol. Manage. 257, 1324–1332.
Saiz, G., Green, C., Butterbach-Bahl, K., Kiese, R., Avitabile, V., Farrell, E.P., 2006. Seasonal and spatial variability of soil respiration in four Sitka spruce stands. Plant Soil 287, 161–176.
Savin, M.C., Gorres, J.H., Neher, D.A., Amador, J.A., 2001. Biogeophysical factors influencing soil respiration and mineral nitrogen content in an old field soil. Soil Biol. Biochem. 33, 429–438.
Scheinost, A.C., Chavernas, A., Barrón, V., Torrent, J., 1998. Use and limitations of second-derivative diffuse reflectance spectroscopy in the visible to near infrared range to identify and quantify Fe oxides in soils. Clays Clay Miner. 46, 528–536.
Scheinost, A.C., Schwertmann, U., 1999. Color identification of iron oxides and hydroxysulfates: use and limitations. Soil Sci. Soc. Am. J. 63, 1463–1471.
Schwendenmann, L., Veldkamp, E., Brenes, T., O'Brien, J.J., Mackensen, J., 2003. Spatial and temporal variation in soil CO_2 efflux in an old-growth neotropical rain forest, La Selva, Costa Rica. Biogeochemistry 64, 111–128.
Singh, B.K., Bardgett, R.D., Smith, P., Reay, D.S., 2010. Microorganisms and climate change: terrestrial feedbacks and mitigation options. Nat. Rev. Microbiol. 8, 779–790.
Souza, C.K., Marques Jr., J., Martins Filho, M.V., Pereira, G.T., 2003. Influência do relevo na variação anisotrópica dos atributos químicos e granulométricos de um Latossolo em Jaboticabal—SP. Eng. Agric. 23, 486–495.
Souza, Z.M., Silva, M.L.S., Guimarães, G.L., Campos, D.T.S., Carvalho, M.P., Pereira, G.T., 2001. Variabilidade espacial de atributos físicos em um Latossolo Vermelho distrófico sob semeadura direta em Selvíria (MS). Rev. Bras. Cienc. Solo 25, 699–707.
Teixeira, D.D.B., Panosso, A.R., Cerri, C.E.P., Pereira, G.T., La Scala, N., 2011. Soil CO_2 emission estimated by different interpolation techniques. Plant Soil 345, 187–194.
Torrent, J., Barrón, V., 2008. Diffuse reflectance spectroscopy. In: Ulery, A.L., Drees, L.R. (Eds.), Methods of Soil Analysis. Part 5. Mineralogical Methods. SSSA Book Series, no. 5. Soil Sci. Soc. Am. J, pp. 367–385.
Vieira, S.R., 2000. Geoestatística em estudos de variabilidade espacial do solo. In: Novais, R.F., Alvarez, V.V.H., Schaefer, C.E. (Eds.), Tópicos em Ciência do Solo. Soc. Bras. Ci. Solo, Viçosa, pp. 1–54.
Viscarra Rossel, R.A., Walvoort, D.J.J., McBratney, A.B., Janik, L.J., Skjemstad, J.O., 2006. Visible, near infrared, mid infrared or combined diffuse reflectance spectroscopy for simultaneous assessment of various soil properties. Geoderma 131, 59–75.

Please cite this article in press as: Bahia, A.S.R.S., et al., Iron oxides as proxies for characterizing anisotropy in soil CO_2 emission in sugarcane areas under green harvest. Agric. Ecosyst. Environ. (2014), http://dx.doi.org/10.1016/j.agee.2014.04.017

Viscarra Rossel, R.A., Webster, R., 2011. Discrimination of Australian soil horizons and classes from their visible-near infrared spectra. Eur. J. Soil Sci. 62, 637–647.
Warrick, A.W., Nielsen, D.R., 1980. Spatial variability of soil physical properties in the field. In: Hillel, D. (Ed.), Applications of Soil Physics. Academic Press, New York, NY, pp. 319–344.
Webster, R., Oliver, M.A., 1990. Statistical Methods in Soil and Land Resource Survey. Oxford University Press, Oxford.
Wollenhaupt, N.C., Mulla, D.J., Crawford, G., 1997. Soil sampling and interpolation techniques for mapping spatial variability of soil properties. In: Pierce, F.J., Sadler, E.J. (Eds.), The State of Site-Specific Management for Agriculture. ASA, CSSA, SSSA, Madison, pp. 19–53.
Xu, M., Qi, Y., 2001. Soil-surface CO_2 efflux and its spatial and temporal variations in a Young ponderosa pine plantation in northern California. Global Change Biol. 7, 667–677.

Please cite this article in press as: Bahia, A.S.R.S., et al., Iron oxides as proxies for characterizing anisotropy in soil CO_2 emission in sugarcane areas under green harvest. Agric. Ecosyst. Environ. (2014), http://dx.doi.org/10.1016/j.agee.2014.04.017